Engineering and Technology Journal
Journal homepage: https://etj.uotechnology.edu.iq

Antibacterial improvement with multilayer of bio-composite coatings produced by electrophoretic deposition

Noor A. Al-Ali*, Makarim H. Abdulkareem, Iman A. Anoon

Production Engineering and Metallurgy Dept., University of Technology-Iraq, Alsina'a street, 10066 Baghdad, Iraq.
*Corresponding author Email:noorkareem772@yahoo.com

HIGHLIGHTS

- Novel multifunctional composite coating layers on a 316 L SS substrate was fabricated
- The first coating layer involves composite of biopolymer (Gelatin with chitosan)
- The second composite coating layer was consist of bioceramic (HA) with chitosan
- Enhanced antibacterial activity and corrosion resistance in the 316 L stainless steel substrate
- Contact angle of the substrate becomes super hydrophilic after coated with multilayer

ARTICLE INFO

Handling editor: Omar Hassoon

Keywords:
Electrophoretic deposition; Gelatin; Chitosan; HA; EPD.

ABSTRACT

In this study, multi-structured coatings of biocompatible and antibacterial materials on a 316 L stainless steel (SS) implant have been electrophoretically deposited for orthopedic applications. Two layers of composite coatings have been deposited; the first layer of composite coating biopolymer layer consists of (chitosan with Gelatin) and the second composite coating layer of bio-ceramic comprises Hydroxyapatite with chitosan. The first layer was deposited at (3 g/L concentration of Gelatin, 20 voltage, and 3 min and 0.5 g/L chitosan) parameters, and the second layer was deposited at (6 g/L, 40 voltage, 1 min, and 0.5 g/L chitosan) parameters. In this study, the stability of the suspension was evaluated using the Zeta potential test, which manifested good stability. The adhesion strength between the composite coatings' first layer and the 316L stainless steel substrate, as well as between the coating layers themselves, was determined using the Tape test, and the removal area for the first layer was 8.06% while for the second layer was 6.01%. The wettability test elucidated for the 316 L stainless steel and first coating layer and the second coating layer, the second composite coating layer became super hydrophilic, and a very high wettability was exhibited with multilayer coating. Scanning electron microscopy showed that the surface's topology revealed a homogenous and defect-free composite coating. The result of the antibacterial efficiency of the 316 L SS substrate improved as the number of coating composite layers increased, and the resistance to corrosion of 316L SS enhanced as the number of coating composite layers increased.

1. Introduction

Metallic materials are one of the artificial implants used in the human body. Among these materials, stainless steel alloy is commonly employed in orthopedic implants, but the type most extensively used in orthopedic implants is 316L stainless steel owing to its elevated mechanical strength [1-4]. Corrosion is important in designing and selecting metals and alloys for service in vivo. Allergenic, toxic/cytotoxic, or carcinogenic species may be released to the body during corrosion processes. In addition, various corrosion mechanisms can lead to implant loosening and failure. In general, metallic implants lack osteoconductivity, resulting in poor adhesion between the implant and the surrounding tissue [5]. Since the biopolymers share chemical properties with the extracellular matrix of many tissues, advantageous biological performance, and cell- or enzyme-controlled breakdown, the biopolymers are increasingly employed in biomedical applications. The advantage of low-temperature processing and coating flexibility is suggested in using biopolymers to create biomedical coatings [6,7].

Chitosan is a natural cationic biopolymer and is always used for biomedical applications due to its non-toxic, antibacterial activity, biodegradable, biocompatible, and hemostatic. Its structure permits specific adjustments without numerous problems. However, chitosan has a disadvantage, as bone formation requires a long time, and crosslinkers are needed to maintain the structure integrity [8]. Gelatin is another type of natural biopolymer with the advantage of being biocompatible, biodegradable, low antigenicity, and virtuous cell recognition. In contrast, the disadvantage of Gelatin is that it involves a fast degradation rate

http://doi.org/10.30684/etj.2023.143475.1588
Received 19 September 2023; Received in revised form 22 November 2023; Accepted 28 November 2023; Available online 08 January 2024
2412-0758/University of Technology-Iraq, Baghdad, Iraq

in physiological fluids and brittleness [9]. Adding Gelatin to chitosan as a composite coating layer improved the usefulness of the chitosan coating for biomedical applications, including control over degradation, drug release profile, and the stimulation of cellular responses. Moreover, when mixed with Gelatin, chitosan will give a composite coating layer with a high coating lifetime due to the high cross-linking degree of Gelatin.

Gelatin's disadvantages include a fast physiological fluid degradation rate and brittleness. Hence, when embedded in a chitosan matrix, these properties are used in biomedical applications [10]. The biocompatibility, such as (cell adhesion and proliferation), was modified when Gelatin was combined with chitosan as a composite coating layer deposited by the EPD technique due to the excellent cell affinity of Gelatin [11]. Hydroxyapatite (HAP) has been employed as a covering for metallic body implants because of its biocompatibility, bioactivity, and closeness to the chemical structure of the inorganic component of bone tissue [12,13]. The composite of organic (biopolymer) –inorganic (bioceramic) coatings were formed effectively when chitosan was combined with the hydroxyapatite component. This will lead to mimicking the human bone. Generally, the best connection between substrate and layer coating was made by the chitosan, which also serves as an excellent layer component binder [14,15]. One of the coating methods is electrophoretic deposition. The electrophoretic deposition technique is a cost-effective colloidal coating technique at room temperature. More than one component can be deposited simultaneously in a single coating step, thus enabling the development of multifunctional coatings [16-18]. The deposition of the first composite coating layer (Gelatin with chitosan) and second composite coating layer (HA with chitosan) by electrophoretic deposition (EPD) process has been successfully carried out on a 316L stainless steel substrate for forming a stable as well as crack-free film with good biological properties and corrosion resistance.

Makarim et al. [19] studied HA with chitosan on SS316L by EPD with Taguchi approach to producing bioceramic nanocomposite coatings on the 316L stainless steel substrate. Matrix coatings, nano-hydroxyapatite (HA), and stabilized zirconia nano yttria (YSZ) with functionally Graded Materials (FGMs) were used. The biopolymer (chitosan) was placed on the 316L stainless steel layer. Different parameters were used to deposit single and nano biocomposite FGM coatings, including (voltage, time, percent concentration of powders, and temperature). Different pH values of (3.5, 4, and 5) and different solvents (ethanol, methanol, n-butanol, and isopropanol) were used to choose the required solvent. The contact angle measurements showed the coating surfaces were hydrophilic and super hydrophilic (62.59°- 2.48°). The samples depicted strong antibacterial activity. Jasim et al., [20] used the EPD process to deposit organic/ inorganic composite coatings on Ti6Al4V alloy substrate (FGM), which consists of HA, YSZ, and titania using chitosan as a binder for orthopedic and dental applications.

They found that all materials used for coating are biocompatible with the human body by implanting them in an in vivo test. Mathina et al. [21] used the EPD process to coat 316L SS substrate by multifunctional biocomposite composed of crab shell derived hydroxyapatite (CSH)- aloe vera (AV)/strontium oxide (SrO)/polyhydroxybutyrate (PHB) composite to enhance antibacterial, mechanical, and biocompatible properties for orthopedic applications. The composite coating of CSH-AV/SrO/PHB has good biological properties for orthopedic applications. Vaez et al., [22] developed new nano-composite coatings of chitosan/ baghdadite for deposition on 316L SS substrate by the EPD. For orthopedic implants, appropriate biological properties were provided by this type of coating. The current study aims to create multifunctional composite coating layers on 316L stainless steel substrate with good characteristics in biomedical applications. The electrophoretic deposition technique was used to deposit the first composite biopolymer coating layer of chitosan with Gelatin and the second composite coating layer of HA with chitosan. A new biological system with good adhesion strength, good antibacterial activity, and corrosion resistance was produced.

2. Experimental work

2.1 Materials

1) 316L stainless steel used as the substrate has the chemical composition listed in Table 1. The chemical analysis used an optical emission spectrometer (OES) type (Foundry-Master x pert 52Q0080) available in the Central Organization for Standardization and Quality Control in Baghdad - Iraq.
2) Two types of biopolymer were used ((Gelatin type B purchased from CDH, and Chitosan (medium molecular weight with a degree of the deacetylation of about 85% soluble in 1% acetic acid) (purchased from Sigma Aldrich)).
3) Bio-ceramic (Hydroxyapatite less than 40 nm purchased from Sky Spring Nanomaterials, USA).
4) (Deionized water, solvents of ethanol absolute (99.9%), and acetic acid with purity (99.5%)).

Table 1: Chemical composition of 316L stainless steel

Element swt.%	**%C**	**%Si**	**%Mn**	**%P**	**%S**	**%Cr**	**%Mo**	**%Al**	**%Ni**	**%Co**	**%Cu**	**%Nb**
wt%	0.015	0.578	1.35	0.043	0.008	16.8	1.79	0.003	9.35	0.221	0.244	0.005
Elements	**%Ti**	**%V**	**%W**	**%Ta**	**%N**	**%Sn**	**%Pb**	**%Se**	**%Sb**	**Others**	**%Fe**	
wt.%	0.011	0.039	0.037	>0.01	0.041	0.011	0.003	0.003	>0.003	>0.001	remain	

2.2 Sample preparation

In this work, the sandblasting process was employed as a surface modification method to increase the roughness of the samples, ensuring optimal adhesion strength of the coating layers. Stainless steel 316L electrode plates were initially cut into dimensions of 2*10*2 mm using a wire-cut machine. The electrode plates were then subjected to ultrasonic cleaning with ethanol followed by acetone for 1 hour. Prior to the electrophoretic coating procedure, the plates were dehydrated. All coatings in this

study were produced using the electrophoretic deposition (EPD) technique. The electrophoretic deposition cell used in this investigation consisted of two electrodes immersed in the beaker containing suspension used for coating. The stainless steel 316L substrate was used as a cathode and anode electrodes (working and counter). Between them, the steady gap was 10 mm when immersed in suspension. Acetone was used to wash the electrodes, and the electrodes were dehydrated. The deposition was performed by immersing the electrode into a beaker filled with the suspension of materials required for coating. Figure 1 illustrates the electrophoretic deposition cell coating 316L stainless steel substrate. Different coating times were employed throughout the experiments, as the digital timer was utilized to determine the necessary duration for each experiment. Additionally, raising and lowering the electrodes was done electrically, and fixing the electrodes was carried out upon the design basis concerning the regime of cell deposition.

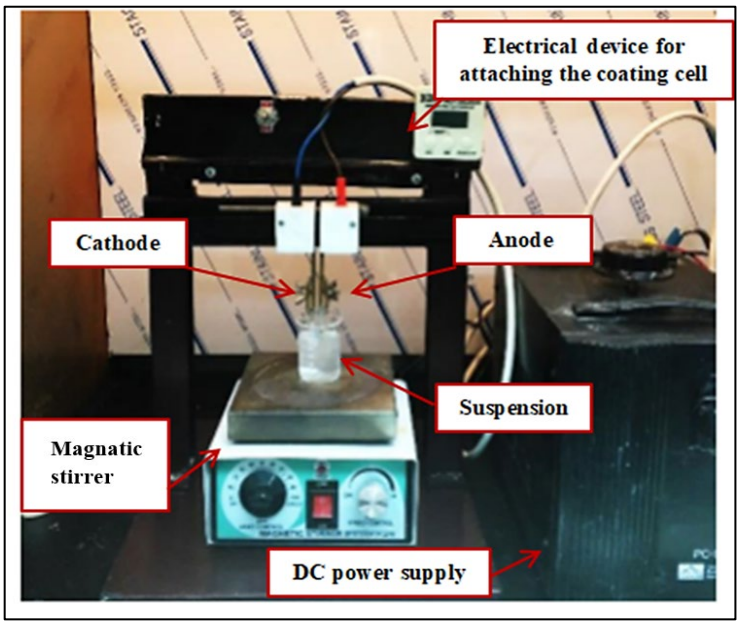

Figure 1: Used EPD system for depositions

2.3 Suspensions preparation for two composite layers

The mechanism of deposited multilayer by EBD technique is shown in Figure 2. In the first stage, the suspension of composite biopolymer was prepared for the first layer and left for 24 hours at room temperature to dry. The second layer of HA with chitosan was deposited from the prepared suspension of HA with chitosan on the first composite coating layer.

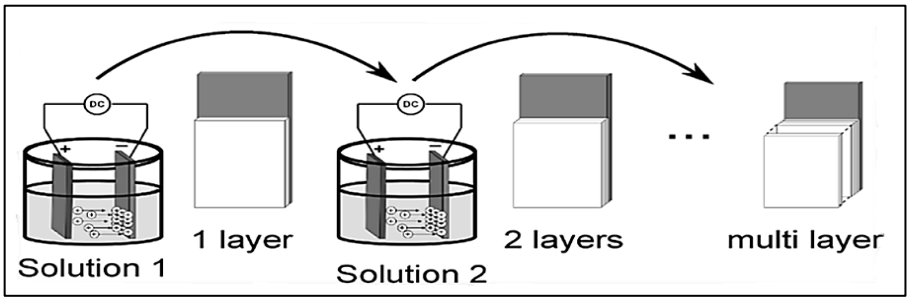

Figure 2: Schematic of the two composite coating layers produced by the EPD technique

2.4 Suspension preparation of gelatin-chitosan for composite coatings layer

The significant stage in the EPD investigational process is the preparation of aqueous suspensions. Gelatin and chitosan suspensions were prepared individually and blended to prepare the gelatin-chitosan composite suspension for the EPD process. A magnetic stirrer melted chitosan powder of (0.5 g/L) into (1 Vol.%) of acetic acid. Then, ethanol was supplemented with the chitosan solution, and the suspension was kept at stirring. Separately, (3 g/L) concentration of gelatin powder was supplemented to (40 Vol.%) of deionized water and (1 Vol.%) of acetic acid. The dissolution was performed via magnetic stirring at (50 ^{o}C) for (1 hour) based on the initial experiments and the determined proper temperature. A hot plate stirrer (MS300HS, MS200) was used. Later, the suspension was smoothly cooled to room temperature beneath the magnetic stirring. Eventually, (59 Vol.%) of ethanol was supplemented to the solution of Gelatin, and the suspension was kept at stirring for 1 hour. The percentage of water and ethanol for gelatin preparation was determined after many initial experiments. The prepared gelatin and chitosan solution was blended at stirring for 2 hours. Then, the suspensions were mixed ultrasonically (Ultrasonic Processor, MIXSONIX Incorporated N.Y, USA) for (0.5 hours) to disperse the solid particles. The parameters for depositing the composite biopolymer coating layer were (3 min) and (20 V).

2.5 Suspension preparation of the second layer (ha with chitosan)

Different concentrations (6, 8, and 10 g/L) of HA powder were used based on initial experiments to determine the best concentration of HA powder to obtain a uniform second composite coating layer. HA suspensions were prepared by dissolving different concentrations of HA powder in deionized water. (0.5 g/L) chitosan powder was melted into (1 Vol.%) acetic acid by a magnetic stirrer, and then ethanol was added and remained on a magnetic stirrer. The suspensions of chitosan and HA were mixed and kept on a magnetic stirrer. The suspensions of HA and chitosan were mixed ultrasonically for (30 min) to disperse the solid particles. Then, the second layer was deposited based on initial experiments; the concentration, time, and voltage were also determined. The best concentration of HA powder was 6 g/L. The parameters to deposit the second layer were (1 min) and (40 V).

3. Method

3.1 Characterization techniques

3.1.1 Zeta potential

The whole suspension's electrophoretic mobility distributions were measured using particle electrophoresis equipment and assessed with regard to zeta potential to ensure both the stability of the colloidal suspension and the coating homogeneity. Zeta potential indicates if the deposition of coating layers was cathodic or anodic. All samples were diluted in a particular liquid prior to testing to ensure the stability of the suspension, and at room temperature, the zeta potential test was performed using (Brookhaven Instruments, ZetaPlus, USA). The diameter hydrodynamic of particles can be identified by the luminous shed laser on the specimens, which will lead to understanding the velocity of diffusion particles. This test was done in the Ministry of Science and Technology. Before testing, the suspension was processed ultrasonically for thirty minutes after magnetic stirring, and then the measurement was done.

3.1.2 Tape test

According to ASTM D3359 [23] as shown in Table 2, a removing pressure-sensing stripe is placed on previously arranged cut lines in a coating film and removed to assess the coatings' adhesion to metallic surfaces. There are two methods of tape testing (cross-hatching testing): A and B. The technique B is used for field testing, while method A is normally employed in laboratories. Despite being frequently utilized, this test tends to be more qualitative. The test was carried out at the University of Technology's Production Engineering and Metallurgy Department, and the outcomes provide numerous levels of visual diagrams for the film pull-off test that were compared with the ISO Class: (0-5)/ASTM:(5B-0B) standard charts.

Table 2: Illustration of the standard ASTM D3359-B

Description	ASTM
The edges of the cuts are completely smooth; none of the squares of the lattice is detached.	5B
Detachment of flakes of coating at the intersections of the cuts. Across cut areas, not significantly greater than 5% is affected.	4B
The coating has flaked along the edges and /or at the intersections of the cuts. Across the cut area, not significantly greater than 5% but not significantly greater than 15% is affected.	3B
The coating has flaked along the edges of the cuts partly or wholly in large ribbons and /or partly or wholly on different parts of the squares. Across the cut area, not significantly greater than 15%, but less than 35% is affected.	2B
The coating has flaked along the edges of the cuts partly or wholly in large ribbons and /or partly or wholly on different parts of the squares. Across the cut area, not significantly greater than 35% but not significantly greater than 65% is affected.	1B
Any degree of flaking that cannot be classified even by classification 1B.	0B

3.1.3 Microstructural examination

The topography of the coating surface was analyzed by FE-SEM. SEM revealed the microstructures and the spreading of the different deposited coatings' constituents. Samples were sputter coated by gold before SEM observation to prevent the charging influence upon the specimens.

3.1.4 Contact angle

At room temperature and ambient humidity, the sessile drop method was used on a drop-shape analysis system (CAM110, China) to measure the static water contact angles and identify the hydrophilic characteristics of the sample surface. The assessed materials are preferred to follow ASTM D7334-08 [24], which involves placing microliter-sized drops of deionized water on a sample surface to determine the static contact angle. The contact angle at the droplet's border reveals the surface's wetness. The University of Technology in Iraq's Chemical Engineering Department gave the test.

3.1.5 Antibacterial activity test by zone inhibition method

The Biotechnology Branch-Nanotechnology Center Laboratory provided samples for testing gram-negative bacteria, including E. coli. In a temperature-controlled environment, these bacteria were cultured on "nutrient agar (N. agar)" and

incubated for (24 hr) at (37°C). They were mixed with 50 ml of normal saline solution to create a "107 FU/ml" bacterial suspension that served as a control, and 100 ml of this solution was poured onto a nutrient agar plate for further examination. Samples of polymers, mixtures, and composites were put onto the plates to identify the inhibitory zone. After some time, these plates were incubated at a temperature of 37°C. After a 24-hour incubation period, the zones of inhibition were identified.

3.1.6 Corrosion test

To illustrate the specimen corrosion in SBF, electrochemical measurements relating to the coated and uncoated samples were performed using a potentiostat/galvanostat (Electrochemical CHI 604 e CorrTest workstation, China). A multiport corrosion cell kit with a capacity of 650 mL was used to test the tested samples according to the standards ASTM G1-03 [25] and ASTM G5-94 [26]. Three electrodes were traditionally employed: Saturated calomel (SCE), which served as the reference electrode, platinum platelet as the counter electrode, and the specimen as the working electrode (WE). Cyclic potentiodynamic test: It was done in the electrolyte of simulated body fluid at 37°C using a potential range from -0.400V to +2.8V and then from +2.8V to -0.400V versus OCP (rate of scanning was 20 mV/s). The size of the hysteresis loop, which is a direct indicator of the kinetics of pit propagation, is another goal. The corrosion rate is evaluated utilizing the mpy approach through the next Equation 1:

$$\text{Corr. Rate} = 0.13 \times i_{\text{corr}} \times \frac{EW}{D} \quad (1)$$

where: Corr. Rate: The rate of corrosion (mpy) Icorr: The current density of corrosions (mA.cm^{-2}) Protection efficiencies (PE%) of all layers of composite coating are estimated by using equations:

$$PE\% = \frac{(icorr)\ uncoated - (icorr)\ coated}{(icorr)\ uncoated} \times 100\% \quad (2)$$

where icorr (uncoated) is the uninhibited current density, and icorr (coated) is the inhibited corrosion current density.

4. Results and discussion

4.1 Solution stability (Zeta potential) results

4.1.1 Zeta Potential test

The zeta potential method was used to examine the stability of coated suspensions, and the findings show that all suspensions with acidic values had positive zeta potential values. Hence, an important factor that should be considered is the suspensions' pH because it strongly affects zeta potential. The pH value was adjusted for all suspensions to stabilize the suspensions, and this led to homogenous dense layers of composite coating. The positive zeta potential is obtained at low pH levels, while at high pH values, the zeta potential value will be negative [27]. In colloidal solutions with high zeta potential, the electrical charge up to the surface of the particles is larger, increasing the electrostatic repulsion between the particles as well. Conversely, the colloidal solutions with a low ζ potential try to coagulate or flocculate [28].

So, to obtain a homogenous composite coating layer, the interaction between the negative and positive materials charge or, in other words, the ability of positive charge materials round the negative charge materials by drawing it to cathodic deposition. The negative zeta potential (-26.81 mV) and mobility (-0.53 (m/s) (V/cm)) of gelatin particles were exhibited in the deionized water as shown in Table 3 and Figure 3 (a and b). The suspension of gelatin with chitosan suspension at pH 4.8 shows cathodic deposition by a positive zeta potential of (77.38 mV) and mobility (1.54 (m/s) (V/cm)) as shown in Table 3 and Figure 4 (a and b). There was a good dispersion of particles into the suspension, so the cathodic EPD coating deposition was achieved when suspension of gelatin was mix with chitosan suspension. High electrical mobility, high oil potentials, and high charges of HA nanoparticles may be produced by utilizing chitosan as a binder [20]. Zeta potential and mobility of the suspension of second layer (HA+ chitosan) were (28.71 mV) and(0.57 (m/s) (V/cm)) as shown in Table 3 and Figure 5 (a and b). There's a vitreous distribution of the particles of HA in the solution of chitosan. The pH for suspension (HA+ chitosan) was (4.9).

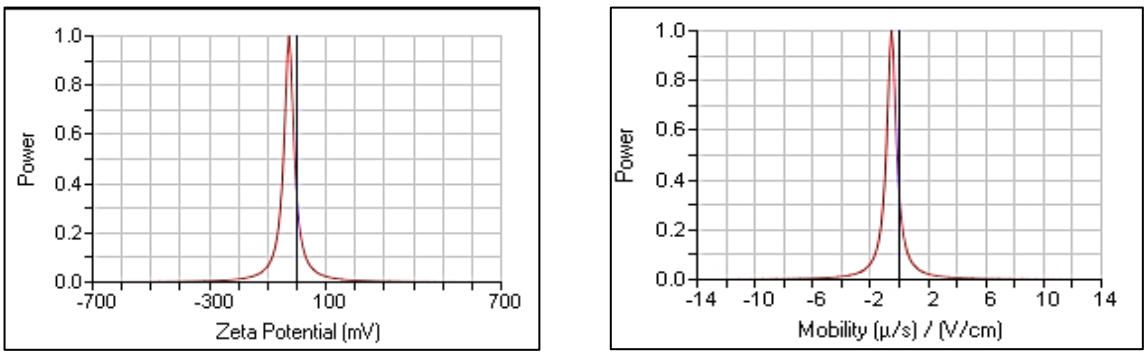

(a) **(b)**

Figure 3: (a) ζ potential and (b) mobility of Gelatin in deionized water

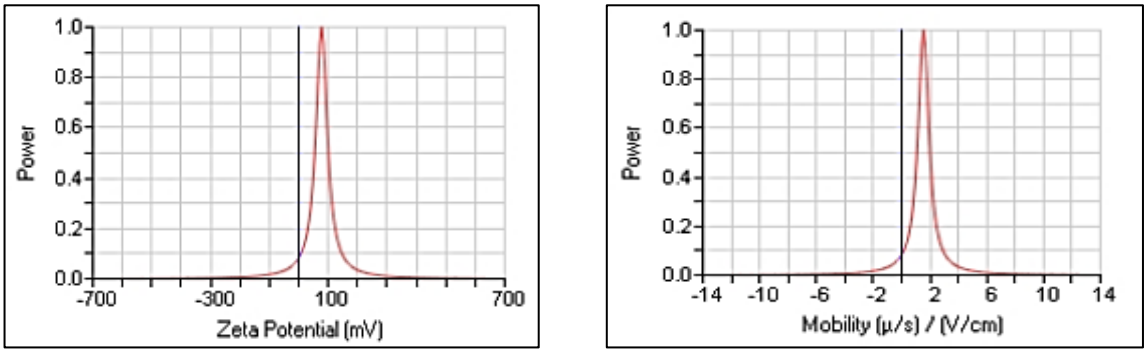

(a) **(b)**

Figure 4: (a) ζ potential and (b) mobility of Gelatin in chitosan suspension

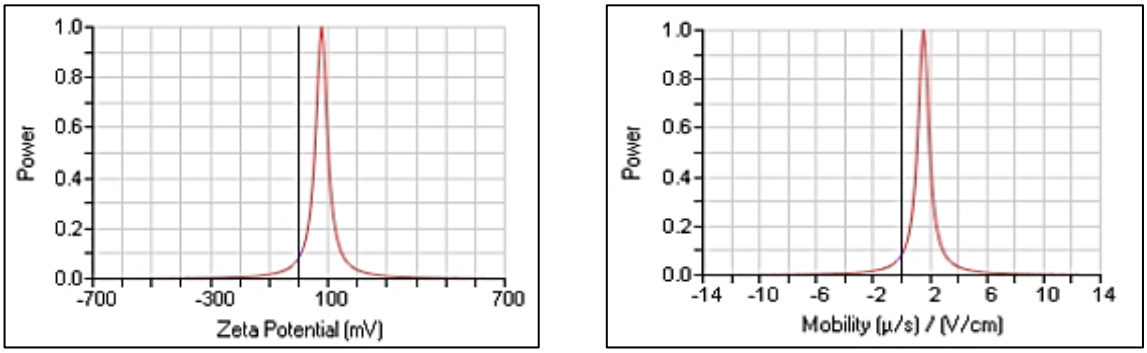

(a) **(b)**

Figure 5: (a) ζ potential and (b) mobility of HA in chitosan suspension

Table 3: Values of zeta potential and mobility for different solutions

Suspension type	Zeta potential (mv)	Mobility (m/s) (V/cm)
Gelatin in deionized water	-26.81	-0.53
Chitosan	30.78	0.61
Gelatin in chitosan	77.38	1.54
HA in chitosan	28.71	0.57

4.2 Adhesion strength test results

The adhesion strength significantly affects the implant's long-term stability [29]. Such strength tests have been used to evaluate the composite coating layer quality. Thus, it was important to study the strength adhesion of such a layer. So, the tape test technique was utilized for such a goal per the ASTM standard (D3359-B). The adhesion strength test was done on the biopolymer composite's first layer and HA's second layer with chitosan. The results showed that all coating layers give good adhesion strength with a substrate and with second layers. Chitosan is utilized as dispersion, charge additive, and an interfacial bonding enhancer since it makes it possible to make well-adhered coatings at ambient temperature. Makram et al. proved this conclusion [30].

The composite coating biopolymer layer provided good adhesion strength with a substrate and a removal area percentage of (8.06%) as shown in Figure 6 (a). In comparison, the removal area percentage was (6.01%) as shown in Figure 6 (b), according to ASTM D3359, and the amount of removed material was 15% or less, which qualified it for ISO class 3/ASTM (3B).

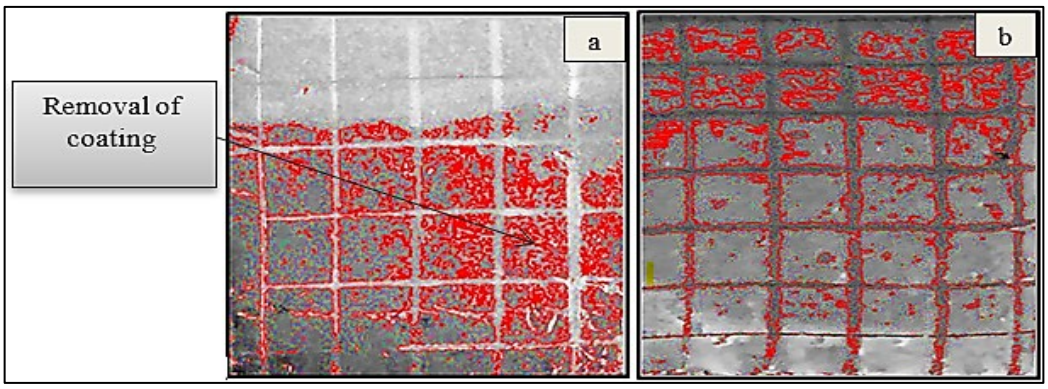

Figure 6: Optical images of removal area percentage for (a) First composite coating biopolymer and (b) second composite coating layer

4.3 Wetability results

When a solid and liquid come into contact, the contact angle (wettability) measurement demonstrates the degree of wetness [30]. Given the link between the two parameters, it is crucial because a smaller contact angle denotes a more biocompatible material [31]. The contact angle is an important factor in biomedical applications because the wettability of the coating plays a crucial role in determining the cell behavior on the biomaterial interaction. The contact angle of the uncoated sandblast substrate was (94.39°) as shown in Figure 7 (a), while the contact angle of the first biopolymer composite coating first layer was (59.50°) as shown in Figure 7 (c). This means that the contact angle of the chitosan layer (82.59°) reduced when gelatin was added to chitosan as shown in Figure 7 (b), while for the second layer of bio-ceramic (HA with chitosan), the contact angle was (18.31°) as shown in Figure 7 (d). From Table 4 and Figure 7 (a,b,c, and d), the uncoated samples had a contact angle of greater than 90°, and after coating with a multilayers, this angle significantly decreased, indicating that the surfaces had changed from hydrophilic to super hydrophilic coating [32]. There are many reasons for this sudden drop in angle value, but the coating's porous structure is the main one [33]. It is believed to gain advantages from nutrients and cell attachments that help form the bones, where the coating's porous nature may cause an extremely rapid water droplet penetration [20]. The second component that might impact the wettability is the surface area, and the second layer of nano HA's increased hydrophilicity (surface wettability) due to its larger surface area since earlier studies have connected the greater surface energy of nanostructured materials to an increase in the adsorption of hydrophilic proteins (like fibronectin) that support the osteoblast density [34]. Adding bio-ceramic to biopolymer led to a decreased contact angle beyond the supplementation, which exhibited the augmented hydrophilic nature of the composite coating. This result is in agreement with [35].

Table 4: Contact angle of samples

No	Type of coating	Contact angle (º)
1	316 L stainless steel (base)	94.39
2	Chitosan layer	82.59
3	The first layer of composite coating biopolymer	59.50
4	The second layer of the second bio ceramic system	18.31

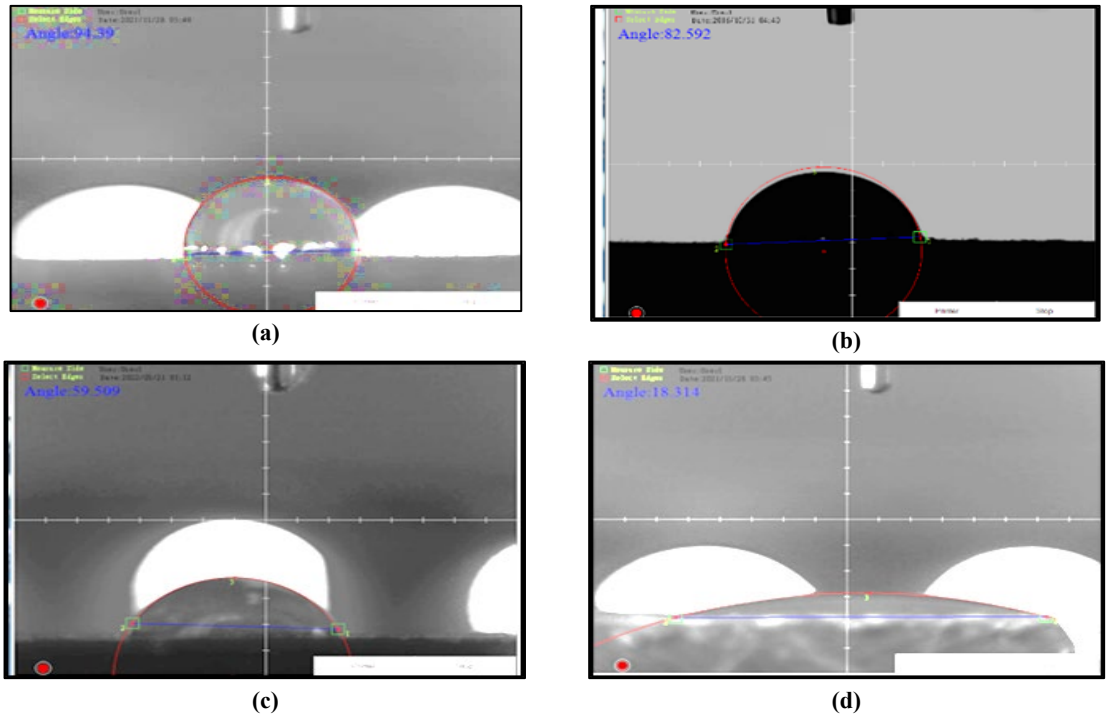

Figure 7: Contact angle image of the uncoated and coated 316L staeinless steel substrat

4.4 Scanning electron microscopy (SEM) results

SEM was utilized to determine the topology of the surface layer for the multilayer composite coating. A homogenous coating was obtained due to the homogenous distribution of particles, as elucidated in Figure 8. At the high magnification. There were no holes and cracks in the coating surface owing to the existence of chitosan as an active binder in the coatings Molaei et al. [36]. The coating surface will appear more uniform and homogenous when the suspension is more stable. This hypothesis coincides with coated samples, where each coating layer's suspension has the highest zeta potential value and is therefore thought to be the most stable suspension [35].

When employing the EPD process, the following factors can affect the coating quality on the zeta potential dependent: Deposition duration, application of voltage, concentration of suspension [37], current flowing through the sample, suspension aging [38], and suspension stability. Although all of the previously mentioned factors significantly affected the coating behavior, the zeta potential was the key factor that substantially affected it [20].

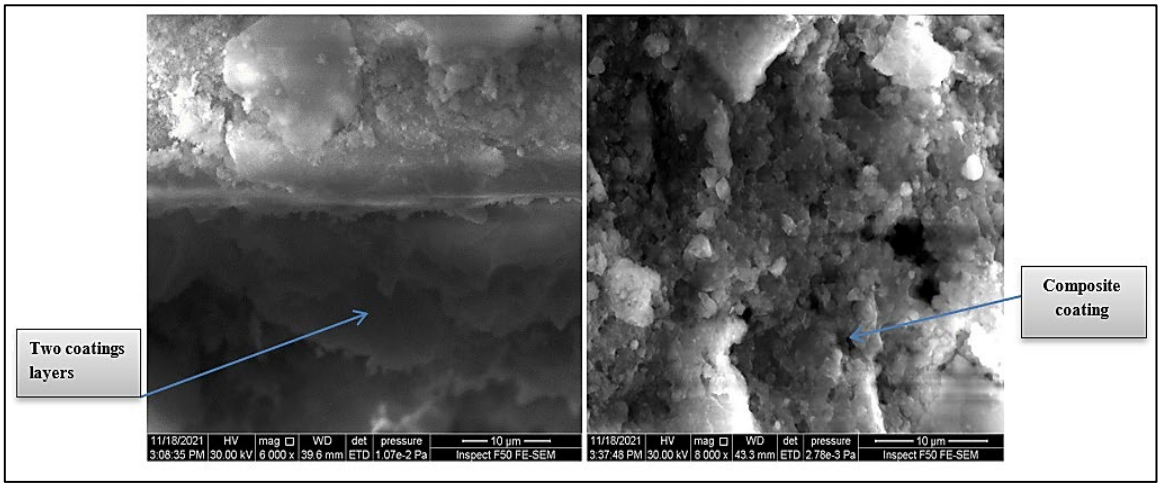

Figure 8: SEM for coated 316L stainless steel substrate

4.5 Antibacterial assessment

Generally, metals and their alloy are not bioactive. This problem leads to bacterial colonization on the implant surface, where the bacteria form a biofilm, and this will lead to the infection of the bone and surrounding tissues, leading to the implants failing following the orthopedic surgeries [39]. The agar disk-diffusion method provided antibacterial properties for the uncoated 316L SS substrate, the first layer of composite coating biopolymer, and the second, as demonstrated in Table 5 and Figure 9. Numerous colonies of bacteria are visible every hour, and the bacteria quantity doesn't reduce with time, depicting the non-antibacterial conduct of the substrate of stainless steel (316L) material. The first layer of composite coating biopolymer gives a better antibacterial effect because the chitosan itself is antibacterial. Therefore, the chitosan-gelatin composite coating layer shows good antibacterial activities compared to the uncoated substrate, which makes them used in biomedical applications. Still, the deposited second layer portrayed a better antibacterial activity than the first layer. It indicated the HAp nanoparticles' strong and broad-spectrum antibacterial activity and their prospective use in the medicinal and environmental domains.

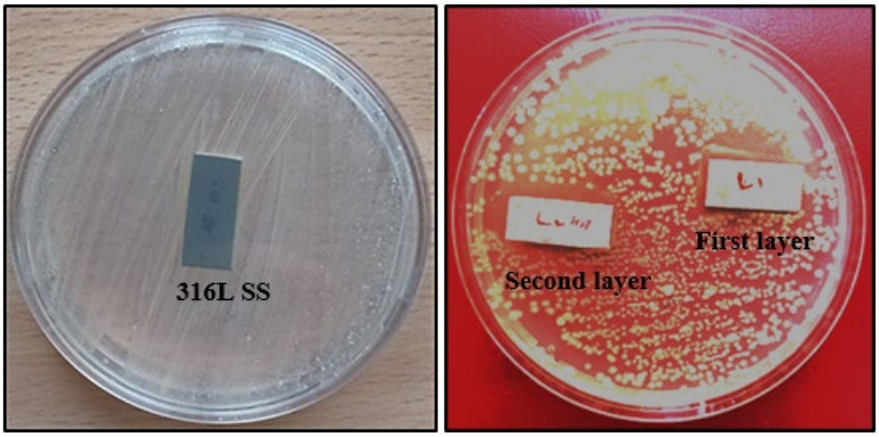

Figure 9: The images for E.coli bacteria by Agar disk-diffusion method for coated and uncoated samples

Table 5: Inhibition zone against E. coli for uncoated and coated samples

Coating type	Zone of inhibition (mm)
316 L stainless steel (base)	
The first composite coating layer	14
The second composite coating layer	18

4.6 Electrochemical bio-corrosion

The major problem in permanent implants is toxicity. Toxicity happens due to releasing ions from the substrate due to the nature of the human body's biological environment—corrosion products' toxicity results from wear and fretting debris. The 316L SS substrate has good corrosion resistance and is always used in nonimplantable and implantable medical devices. The biological environment of the human body is corrosive to metals since it is ionic. Also, wear debris is a major problem of metallic alloy in the human body. The release of ions and debris harms the organs and tissues. One of the methods that help protect the metals and their alloys from aggressive attack in the human body environment is the coating method. The polarization curves have been regarded for the uncoated substrate and biopolymer composite coating.

From Table 6, it can be noted that the corrosion decreased with biopolymer composite coating layers, where the corrosion rate decreased from (6.303×10^{-2} mmpy) for the uncoated 316L stainless steel sample to (4.411×10^{-2} mmpy) for the coated sample with the composite coating layer; this means the corrosion rate decreased with the composite coating layer than the uncoated sample. Also, it can be noticed from this table that the open-circuit potential (OCP) value decreased from (-0.491 volt) for the uncoated 316L stainless steel sample to (-0.423 volt) for the coated sample, while for the second coating layer, the OCP value was (-0.413 volt). Additionally, the corrosion rate decreased from (4.411×10^{-2} mmpy) for the coated sample with the composite coating layer to (3.332×10^{-2} mmpy), indicating that the sample with coating becomes more passive.

Table 6: Corrosion parameters obtained from the tests of corrosion for the uncoated alloy of 316L stainless steel and coated sample

Sample	Eb (volt)	Erep (volt)	OCP (volt)	E corrosion (V)	I corrosion (Amp)	Corrosion rate (mmpy)	Protection efficiency %
316 L stainless steel substrate (BASE)	2.169	0.042	-0.491	-0.692	2.1863×10^{-6}	6.303×10^{-2}	
The first layer of composite coating (Gelatin)	2.900	0.410	-0.423	-0.602	1.530×10^{-6}	4.411×10^{-2}	30%
The second layer of composite coating (L2HA)	3.228	0.372	-0.413	-0.614	1.155×10^{-6}	3.332×10^{-2}	47%

From Figure 10, it can be seen clearly that the uncoated sample (base) has a very wide hysteresis loop, the potential breakdown point (Eb) for the uncoated sample is (2.169 volts), and the re-passivation potential (Erep) is (0.042 volt). At the same time, it can be noted that the potential breakdown point (Eb) and (Erep) for the composite coating layer are (2.655 volts) and (2.900 volts), respectively, and for the second coating layer, the (Eb) and (Erep) are (3.228 (0.372 volts), respectively. This means the breakdown potential was raised by about (0.33 volts) for the composite coating second layer sample than the uncoated sample. Accordingly, it can be concluded that the composite coating layer delayed the breakdown of the passive layer. Also, that means the composite coating layer of the sample had a passive layer that was quickly rebuilt.

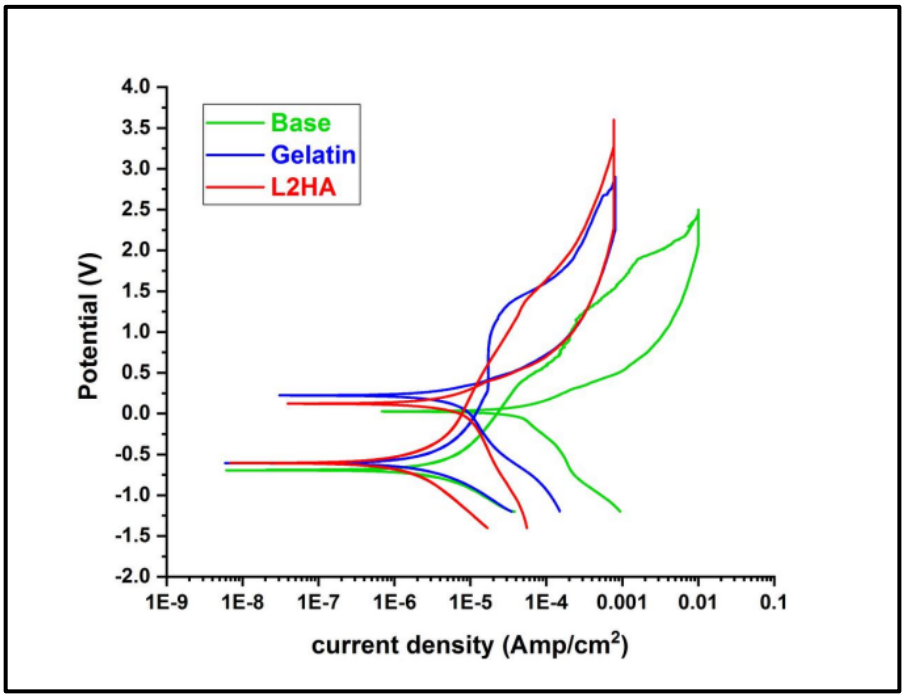

Figure 10: The polarization curves for the composite coating layers (316L SS substrate, First layer , and Second layer)

5. Conclusion

1) The optimum deposition conditions for the composite coating first layer were determined with 20 V applied voltage, 3 minutes deposition time, concentration of 0.5 g/L chitosan, and a gelatin concentration of 3 g/L at a temperature of 50 °C. These conditions formed a well-adhered and homogenous coating and a removal area of 8.06% without any cracks.
2) The zeta potential measurements indicated that the gelatin-chitosan coating suspensions exhibited suitable values, promoting the stability and homogeneity of the composite coating. The zeta potential value was (77.38 mv) with (1.54 (μ/s) (V/cm)) mobility.
3) The contact angle measurements revealed a decrease in the contact angle of the coated 316L SS substrate compared to the uncoated surface. This suggests that the composite coating layer improved the surface hydrophilicity, which is

beneficial for cell adhesion and biocompatibility. The contact angle of the first biopolymer composite layer was 59.50, while the contact angle for the 316L substrate was 94.39. The chitosan layer was 82.59, where the composite coating biopolymer layer is better than the layer containing one coating biopolymer type.

4) The first layer of composite coating biopolymer shows better antibacterial bioactivity than 316L stainless steel substrate.
5) The composite coating layer significantly increases the corrosion resistance of the 316L SS substrate. The corrosion rate decreased, and the open-circuit potential (OCP) shifted towards a more passive range, indicating enhanced resistance against corrosive attacks in the biological environment. The protection of the first composite coating efficiency was 30%.
6) The second bioceramic (HA) layer with biopolymer as the composite system was deposited in parameters of 6g/L concentration of HA with 0.5 g/L of chitosan, 1 min, and 40 volts.
7) The Zeta potential for suspension coating HA with chitosan (28.71 mV) was more stable.
8) The contact angle for the composite coating layer was 18.31. As a result, the sample became extremely hydrophilic after coating the second composite layer.
9) Scanning electron microscopy shows that composite coating layers are homogenous without defects, such as cracks.
10) Antibacterial study results show that the second composite coating layer has better antibacterial activity than the first.
11) The corrosion resistance was increased after the second composite coating layer, and Protection efficiency was 47%

Acknowledgment

The researchers would like to sincerely thank the Production Engineering and Metallurgy Department at University of Technology for allowing us to accomplish such an investigation.

Author contributions

Methodology: Noor. AL- Ali, M. Abdul Kareem and I. Anoon; Writing-Original Draft Preparation, M. Abdul Kareem and I. Anoon. Writing-Review and Editing, Noor. AL- Ali, M. Abdul Kareem and I. Anoon. All authors have read and agreed to the published version of the manuscript.

Funding

The present research has not received any external funding.

Data Availability Statement:

The data supporting the current research results are accessible upon request from the corresponding author.

Conflicts of Interest:

The researchers declare that there's no conflict of interest.

References

[1] C. Kose, R. Kacar, In vitro bioactivity and corrosion properties of laser beam welded medical grade AISI 316L stainless steel in simulated body fluid, Int. J. Electrochem. Sci., 11 (2011) 2762–2777. http://dx.doi.org/10.20964/110402762

[2] S.B. Goodman, Z. Yao, M. Keeney, F. Yang, The future of biologic coatings for orthopedic implants, Biomaterials, 34 (2013) 3174–3183..https://doi.org/10.1016/j.biomaterials.2013.01.074

[3] H.T. Aro, J.J. Alm, N. Moritz, T.J. Mäkinen, P. Lankinen, Low BMD affects initial stability and delays stem osseointegration in cement less total hip arthroplasty in women: a 2-year RSA study of 39 patients, Acta Orthop, 83 (2013) 107–114. .https://doi.org/10.3109/17453674.2012.678798

[4] Gristina, A., Naylor, P., and Myrvik, Q., Biomaterial centered infections: microbial adhesion versus tissue integration, in: T. Wadström, I. Eliasson, I. Holder, Å. Ljungh (Eds.), Pathog. Wound Biomater. Infect. SE-25, Springer, London, (1990)193–216. http://dx.doi.org/10.1007/978-1-4471-3454-1_25.

[5] K. Okuno, M. Sumita, Y. Ikada, and T. Tateishi, The history of metallic biomaterials, Metallic Biomaterials - Fundamentals and Applications, ICP, IARC Monographs on the Evaluation of Carcinogenic Risks to Humans, Surgical Implants and other Foreign Bodies, Lyon, 74 (1999) 65-84.

[6] Z.C. Wang, F. Chen, L.M. Huang, and C.J. Lin, Electrophoretic Deposition and Characterization of Nano-Sized Hydroxyapatite Particles, J. Mater. Sci., 40 (2005) 4955-4957. http://dx.doi.org/10.1007/s10853-005-3871-x

[7] A. Balamurugan, G. Balossier, J. Michel, and J.M.F. Ferreira, Electrochemical and Structural Evaluation of Functionally Graded Bioglass-Apatite Composites Electrophoretically Deposited onto Ti6Al 4V Alloy, Electrochim. Acta, 54 (2009) 1192-1198. https://doi.org/10.1016/j.electacta.2008.08.055

[8] G.S. Kumbar, T. C. Laurencin, and Meng Deng, Natural and Synthetic Biomedical Polymers, Newnes, 2014.

[9] A. Stoch, A. Brożek, G. Kmita, J. Stoch, W. Jastrzębski, and A. Rakowska, Electrophoretic Coating of Hydroxyapatite on Titanium Implants, J. Mol. Struct., 596 (2001) 191-200. https://doi.org/10.1016/S0022-2860(01)00716-5

[10] Y. Liu , B. Zhang, K.M. Gray, Y. Cheng, E. Kim, G.W. Rubloff,W.E. Bentley, Q. Wang, G.F. Payne, Electrodeposition of a weak polyelectrolyte hydrogel: remarkable effects of salt on kinetics, structure and properties, Soft Matter., 9 (2013) 2703-2710. http://dx.doi.org/10.1039/C3SM27581G

[11] J. Song, Q. Chen, Y. Zhang, M. Diba, E. Kolwijck, J. Shao, J. A. Jansen, et al, Electrophoretic Deposition of Chitosan Coatings Modified with Gelatin Nanospheres to Tune the Release of Antibiotics, ACS Appl. Mater. Interfaces, 8 (2016) 13785-13792. https://doi.org/10.1021/acsami.6b03454

[12] B. Ben-Nissan, C. Chai, and L. Evans, Crystallographic and spectroscopic characterization and morphology of biogenic and synthetic Apatites, in Encyclopedic Handbook of Biomaterials and Bioengineering Vol. 1, Part B: Applications, eds. D. L. Wise, D. J. Trantolo, D. E. Altobelli, M. J. Yaszemski, J. D. Gresser, and E.R. Schwartz, (Marcel Dekker Inc., New York,(1995) 191-221.

[13] T. Matsushita, and H. Takahashi, 17- Orthopedic Applications of Metallic Biomaterials, Met. Biomed. Devices, (2019) 431-73. https://doi.org/10.1016/B978-0-08-102666-3.00017-1

[14] Z. Zhang, T. Jiang, K. Ma, X. Cai, Y. Zhou, Y. Wang, Low temperature electrophoretic deposition of porous chitosan/silk fibroin composite coating for titanium biofunctionalization, J. Mater. Chem., 21 (2011) 7705-7713. https://doi.org/10.1039/C0JM04164E

[15] S. Heise, M. Hohlinger, Y.T. Hernández, J.J.P. Palacio, J.A.R. Ortiz, V. Wagener, S. Virtanen, AR. Boccaccini, Electrophoretic deposition and characterization of chitosan/bioactive glass composite coatings on Mg alloy substrates, Electrochim. Acta , 232 (2017) 456-464. https://doi.org/10.1016/j.electacta.2017.02.081

[16] A.R. Boccaccini, S. Keim, R. Ma, Y. Li, and I. Zhitomirsky, Electrophoretic Deposition of Biomaterials, J. R. Soc. Interface, 7 (2010) S581-S613. https://doi.org/10.1098/rsif.2010.0156.focus

[17] C.Valdez, Alejandra, and A. R. Boccaccini, Innovations in Electrophoretic Deposition: Alternating Current and Pulsed Direct Current Methods, Electrochim. Acta, 65 (2012) 70-89. https://doi.org/10.1016/j.electacta.2012.01.015.

[18] L. Besra, and M. Liu, A Review on Fundamentals and Applications of Electrophoretic Deposition (Epd), Prog. Mater. Sci., 52 (2007) 1-61. https://doi.org/10.1016/j.pmatsci.2006.07.001

[19] M. J. Kadhim, N. E. Abdullatef, M.H. Abdulkareem, Optimization of Nano Hydroxyapatite/chitosan Electrophoretic Deposition on 316L Stainless Steel Using Taguchi Design of Experiments, Al-Nahrain J. Eng. Sci., 20 (2017) 1215-1227.

[20] Jasim, A. N. Enhancing The Mechanical Properties and Biological Characteristics of EPD Nano Composites Functionally Graded Organic/Inorganic Systems for Medical Applications, University of Technology Department of Production Engineering and Metallurgy, 2020.

[21] M. Mathina , E. Shinyjoy, S. Ramya, L. Kavitha , D. Gopi a, Multifunctional crab shell derived hydroxyapatite/metal oxide/ polyhydroxybutyrate composite coating on 316L SS for biomedical applications, Mater. Lett., 313 (2022) 131701. https://doi.org/10.1016/j.matlet.2022.131701

[22] S. Vaez, R. Emadi , S. Sadeghzade , H. Salimijazi , M. Kharaziha, Electrophoretic deposition of chitosan reinforced baghdadite ceramic nano-particles on the stainless steel 316L substrate to improve biological and physical characteristics, Mater. Chem. Phys., 282(2022) 125991 . https://doi.org/10.1016/j.matchemphys.2022.125991

[23] D. Mathew, G. Bhardwaj, Q. Wang, L. Sun, B. Ercan, M. Geetha, and T. J. Webster, Decreased Staphylococcus Aureus and Increased Osteoblast Density on Nanostructured Electrophoretic-Deposited Hydroxyapatite on Titanium without the Use of Pharmaceuticals, Int. J. Nanomed., 9 (2014) 1775-1781. https://doi.org/10.2147/ijn.s55733

[24] ASTM D7334-08: Standard practice for surface wettability of coatings, substrates and pigments by advancing contact angle measurement: active standard, Am. Soc. Test. Mater., 08 (2013) 1–3.

[25] Anon, Standard Practice for Preparing, Cleaning, and Evaluating Corrosion Test Specimens., ASTM Spec. Tech. Publ., 90 (1985) 505–510.

[26] ASTM International, G5-14 Standard Reference Test Method for Making Potentiostatic and Potentiodynamic Anodic, 14 (2014) 1–8.

[27] Chapter 10 Microfluidic methods for measuring zeta potential. in Interface Science and Technology, 2 (2004)

[28] D. Predoi, S. L. Iconaru, M.V. Predoi , M. Motelica-Heino, R. Guegan , N. Buton, Evaluation of antibacterial activity of zinc-doped hydroxyapatite colloids and dispersion stability using ultrasounds, Nanomaterials, 9 (2019) 515. https://doi.org/10.3390/nano9040515

[29] P.C. Rattan, B.P.Singh, L. Besra, S. Bhattacharjee, Multiwalled carbon nanotubes reinforced hydroxyapatite-chitosan composite coating on Ti metal: corrosion and mechanical properties, J. Am. Ceram. Soc., 95 (2012) 2725–2731. https://doi.org/10.1111/j.1551-2916.2012.05195.x

[30] M.H. Abdulkareem, , A. H Abdalsalam, and A.J. Bohan, Influence of Chitosan on the Antibacterial Activity of Composite Coating (Peek/Hap) Fabricated by Electrophoretic Deposition, Prog. Org. Coat., 130 (2019) 251-259. https://doi.org/10.1016/j.porgcoat.2019.01.050

[31] T. P. Queiroz , R. S. de Molon, F. Á. Souza, R. Margonar, A. H. A. Thomazini, A. C. Guastaldi, E. Hochuli-Vieira, In Vivo Evaluation of Cp Ti Implants with Modified Surfaces by Laser Beam with and without Hydroxyapatite Chemical Deposition and without and with Thermal Treatment: Topographic Characterization and Histomorphometric Analysis in Rabbits, Clin. Oral Investig., 21 (2017) 685-699. https://doi.org/10.1007/s00784-016-1936-7

[32] Y. Huang, G. Song, X. Chang, Z. Wang, X. Zhang, S. Han, Z. Su, H. Yang, D. Yang, X. Zhang. Nanostructured Ag+-Substituted Fluorhydroxyapatite-Tio2 Coatings for Enhanced Bactericidal Effects and Osteoinductivity of Ti for Biomedical Applications, Int. J. Nanomed., 13 (2018) 2665-2684. https://doi.org/10.2147/IJN.S162558

[33] J. Liu, J. Liue, J. Liu, S. Attarilar, C. Wang, M. Tamaddon, C. Yang, K. Xie, et al., Nano-Modified Titanium Implant Materials: A Way toward Improved Antibacterial Properties, Front. bioeng. Biotechnol., 8,2020,576969. https://doi.org/10.3389/fbioe.2020.576969

[34] X. Shen, J. Wang, and G. Xin, Effect of the Zeta Potential on the Corrosion Resistance of Electroless Nickel and Pvdf Composite Layers Using Surfactants , ACS omega, 48 (2021) 33122-33129. https://doi.org/10.1021%2Facsomega.1c05490

[35] O. Saleem, M. Wahaj, M. A. Akhtar, and M. A.U.Rehman, Fabrication and Characterization of Ag–Sr-Substituted Hydroxyapatite/Chitosan Coatings Deposited Via Electrophoretic Deposition: A Design of Experiment Study, ACS omega, 36 (2020) 22984-22992. https://doi.org/10.1021/acsomega.0c02582

[36] A. Molaei, M. Yari, and M. R. Afshar, Modification of Electrophoretic Deposition of Chitosan–Bioactive Glass–Hydroxyapatite Nanocomposite Coatings for Orthopedic Applications by Changing Voltage and Deposition Time, Ceram. Int., 10 (2015) 14537-14544. https://doi.org/10.1016/j.ceramint.2015.07.170

[37] I. Aydın, A. İ.Bahçepınar, M. Kırman, and M. A. Çipiloğlu, Ha Coating on Ti6al7nb Alloy Using an Electrophoretic Deposition Method and Surface Properties Examination of the Resulting Coatings, Coatings, 9 (2019) 402. https://doi.org/10.3390/coatings9060402

[38] A. Wu, P.M. Vilarinho, and A.I. Kingon, Electrophoretic Deposition of Lead Zirconate Titanate Films on Metal Foils for Embedded Components, J. Am. Ceram. Soc., 89 (2006) 575-581. https://doi.org/10.1111/j.1551-2916.2005.00732.x

[39] A.G. Gristina, Biomaterial-Centered Infection: Microbial Adhesion Versus Tissue Integration, Science, 237 (1987) 1588-1595. https://doi.org/10.1126/science.3629258